Thesis summary

An investigation into the identification and modelling of time-dependent behaviour of deep level excavations in hard rock

D.F. Malan

ABSTRACT

The objective of this study was to understand the mechanisms leading to the time-dependent deformation of deep excavations in hard rock and to develop appropriate numerical techniques to simulate it. Although hard rock is not usually associated with large creep deformation, data collected from the excavations of the deep South African gold mines illustrates significant time-dependent behaviour. The initial part of this study focused on the uniaxial creep testing of quartzite and lava specimens, indicating that the creep rates of these rock specimens are low. These laboratory measurements were compared with closure data collected in underground stopes. The continuous closure data illustrates significant time-dependent behaviour and contains much information that is lost if only daily measurements are taken. This closure behaviour is the result of the rheology of the fracture zone and the time-dependent extension of this zone following a mining increment. An important finding of this study is that continuous closure data provides useful diagnostic information about the stress conditions in the fracture zone ahead of the stope. This may possibly be used to identify hazardous conditions such as areas prone to face bursting. As no previous attempt has been made to simulate the continuous time-dependent closure behaviour of tabular stopes in hard rock, various approaches were investigated. The author developed a viscoelastic convergence solution for the incremental mining of a stope. Both an analytical approach and implementation in a displacement discontinuity program were considered. Although this model gave a good fit to the observed closure behaviour, some problems are associated with this approach as it is unable to simulate the fracture zone. To simulate the time-dependent development of this zone, a continuum viscoplastic approach was developed and implemented in a finite difference code. This proved successful in modelling the time-dependent closure stopes and squeezing conditions in weaker quartzites. As the shear creep of discontinuities may be an important time-dependent mechanism, a laboratory testing program was conducted. Results indicated that discontinuities with gouge infilling undergo noticeable shear creep while the creep rate for mining induced extension fractures is negligible. To simulate this behaviour, a viscoplastic displacement discontinuity technique was developed. This, combined with a tessellation approach, enabled the successful modelling of typical stope closure behaviour and the time-dependent formation of fractures.

1. Introduction

Changes in the local stress state due to mining activity perturb the stability of the rock mass surrounding excavations. The subsequent readjustment of the rock towards a new equilibrium does not occur instantaneously but as a gradual process over time. This process can include two types of inelastic deformation namely "creep-like" movements and violent failures or rockbursts. Depending on the rock type and stress, excavations can show a propensity towards either of these two phenomena. In relation to mine safety, it is important to determine the conditions associated with the transition from stable deformation to rockbursts. Although stable deformation is preferred, excessive "creep-like" rock movements are also undesirable as they may significantly affect the long term stability of underground openings. The rock may deform continuously leading to an eventual collapse. Any engineering design must therefore include the time-dependent properties of the rock. To accomplish these objectives, time-dependent constitutive laws for rock, including hard brittle material, must be established.

To avoid confusion over the terms *creep* and *time-dependency*, the following definitions were introduced and used throughout the thesis. *Creep* is continued deformation due to a constant applied stress and is used exclusively in relation to intact laboratory-sized rock specimens or single discontinuities. *Time-dependency* is continued deformation of the rock mass around mine openings when subjected to a constant far-field stress. Time-dependency is therefore a complex result of the creep of intact rock, creep of multiple discontinuities and the delayed initiation and growth of new fractures. Time-dependency is also understood to refer to deformations not related to geometric changes in the dimensions of an excavation. It occurs on a time scale of days to years and is therefore not related to elastodynamic behaviour.

Creep of rocks has been studied since the early part of the 20th century resulting in the availability of a large amount of data. Most of the studies, however, have focused on the softer saltrocks because they show significant creep under stress and temperature conditions easily applied in the laboratory. For engineering applications, the importance of time-dependent behaviour in the form of rapid convergence of squeezing tunnels in weak rock is well known. In comparison, creep strain in crystalline rock is of limited importance in most engineering projects due to the very low creep rate. An engineering application where the time-dependent behaviour of hard rock recently became more important is the study of the long term stability of chambers used for nuclear waste repositories. An important aspect of the problem is that the excavations must be maintained for several decades to allow retrieval of waste and monitoring of repository performance.

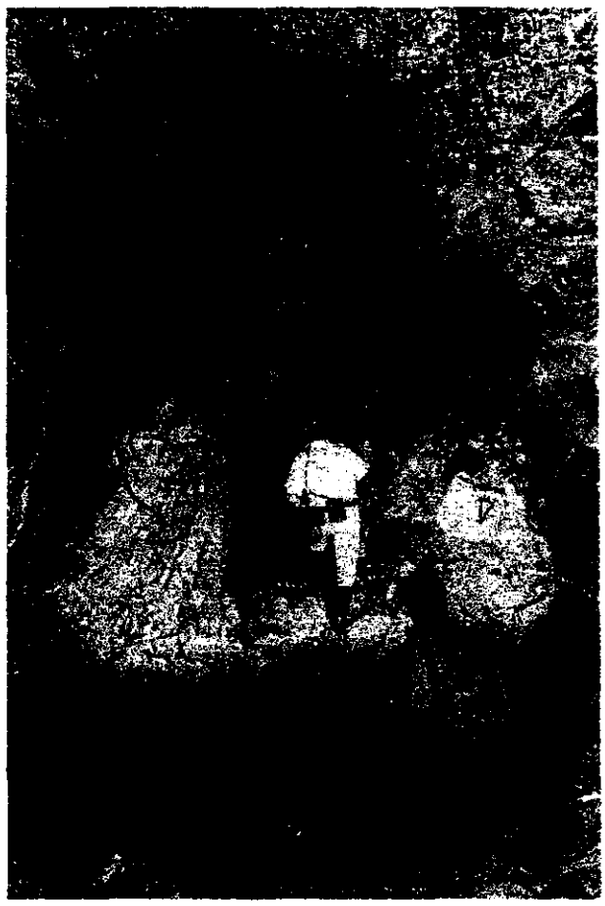

Figure 1. Adverse haulage conditions at Hartebeestfontein Gold Mine in South Africa caused by slow time-dependent deformation processes in the rock. Note that this is not rockburst damage.

2. Laboratory creep of intact hard rock

As no published data was available on the creep of hard rock from the South African mining industry, the first part of the study investigated the laboratory creep of rock specimens from these mines. The samples tested are representative of the rocks found in these mines and are given in Table 1. The objective of this work was to quantify the typical strain rates that could arise when subjecting some of these rocks to constant applied stresses. The tests were conducted on a creep testing machine that uses deadweight loading and cantilevers to maintain a constant uniaxial load on the specimen. The test methodology consisted of loading the same specimen to different stress levels by starting at a low value and increasing the stress in steps, allowing a certain time interval for creep. Although the creep strain rates of these specimens were low, measurable room temperature creep was recorded. Typical primary, secondary and tertiary creep phases were noted. The strain rate of the secondary creep phase

is strongly dependent on stress levels with higher stresses leading to higher creep rates. This behaviour was successfully simulated with a stress power law.

Table 1. Elastic and strength properties of the rock types used in the creep experiments. The abbreviations are: UCS – uniaxial compressive strength, E – Young's modulus, ν - Poisson's ratio.

Rock Type	Location	UCS (MPa)	E (GPa)	ν
Argillaceous quartzite	Lorraine Mine	100	63	0.18
Ventersdorp lava	Western Deep Levels Mine	436	88	0.26
Quartzite	Western Deep Levels Mine	237	79	0.13
Argillaceous quartzite	Hartebeestfontein Mine	142	72	0.26

Figure 2 illustrates the steady-state creep rates for the different rock types at various stress levels. When normalising the data from Figure 2 with respect to the uniaxial compressive strength (UCS) of the particular sample, it appears that the actual strain rate is determined by the ratio of the applied stress σ to UCS and relatively independent of rock type or absolute stress values. This is shown in Figure 3. For the rock surrounding a stope at a particular depth, quartzites with the lower uniaxial compressive strengths will have a higher σ/UCS ratio than lava. From Figure 3 the creep rate of the quartzite under these conditions will therefore be higher. This has implications for the rock mass behaviour of the Ventersdorp Contact Reef stopes in the South African mines where the hangingwall consists of hard lava and the footwall of quartzite. As the ratio of deviatoric stress to failure strength at a particular distance from the excavation will be higher for the quartzite than the lava, creep failure may occur more readily in the quartzite. As stable fracturing dissipates stored energy, this behaviour may be advantageous in reducing violent rockbursts. Mining of the Ventersdorp Contact Reef in areas where the lava is particularly hard can be difficult owing to the rolling nature of the reef. In areas where the reef rolls into the footwall, the mining is sometimes slow to follow, resulting in mining taking place entirely in the lava. The stable formation of the fracture zone is often disrupted leading to face bursting. This phenomenon has been observed at mines in the Carletonville area.

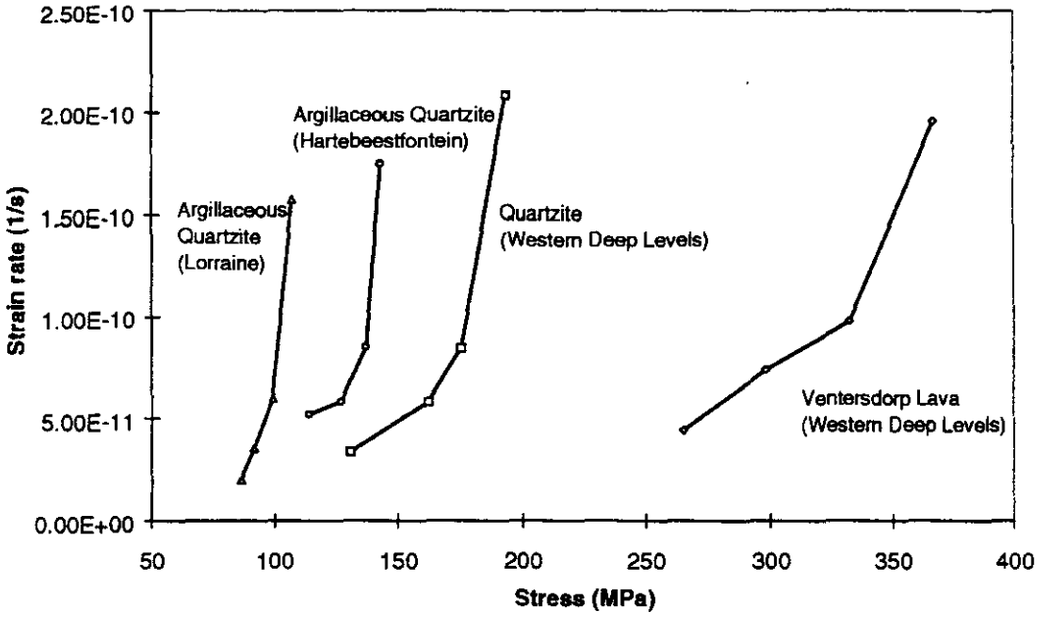

Figure 2. Effect of stress on the steady-state creep rate of different hard rocks in the South African gold mining industry.

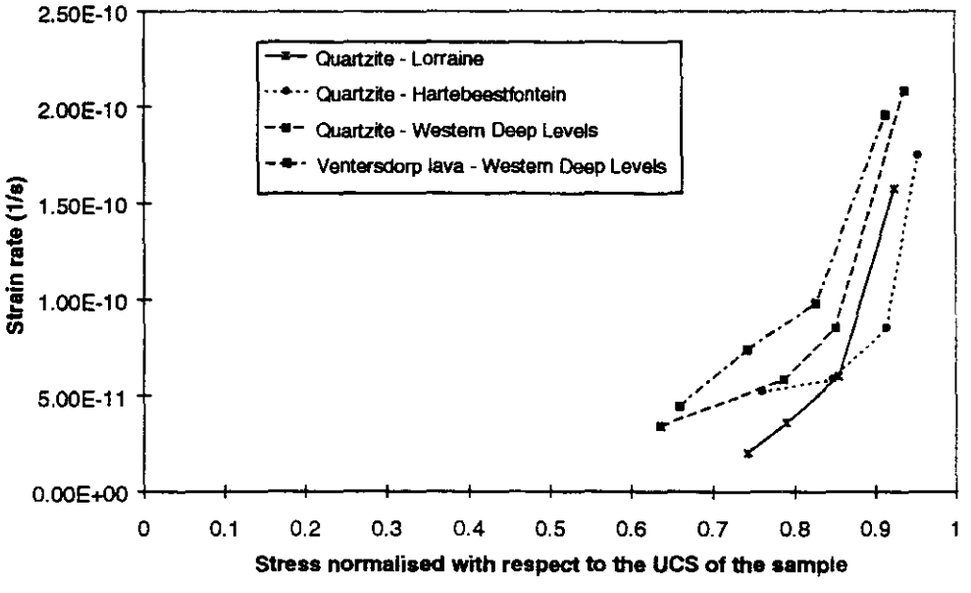

Figure 3. The steady-state creep rate of hard rock as a function of the σ/UCS ra

Further work focussed on use of this data to calibrate a Burgers viscoelastic m The primary and secondary creep phase of these rock samples at a particular loa be successfully simulated with this model. Similar to other rock types. however, the cosity parameters in this model are not fundamental material constants but functions of s . This dependency was investigated and described by an empirical power law.

3. Time-dependent closure measurements

The laboratory creep measurements were contrasted with continuous time-dependent closure measurements in the tabular excavations of the South African gold mining industry. Figure 4 illustrates the face area of a typical panel. Closure is the relative movement of the hangingwall and footwall normal to the plane of the reef (see Figure 5). Various experimental sites were established in stopes in two main reef types of the mining industry namely the Ventersdorp Contact Reef and the Vaal Reef. Stopes in the Ventersdorp Contact Reef are characterised by a lava hangingwall and a quartzite footwall whereas on the Vaal Reef, both the hangingwall and footwall consist of quartzite. The rock mass behaviour of the Vaal Reef is influenced by prominent bedding planes in the hangingwall and footwall. An important finding of this study is that continuous closure data of these stopes contains much information that is lost if the more conventional daily closure measurements are taken. The continuous closure data illustrated significant time-dependent behaviour that cannot be explained by the laboratory creep of intact rock alone.

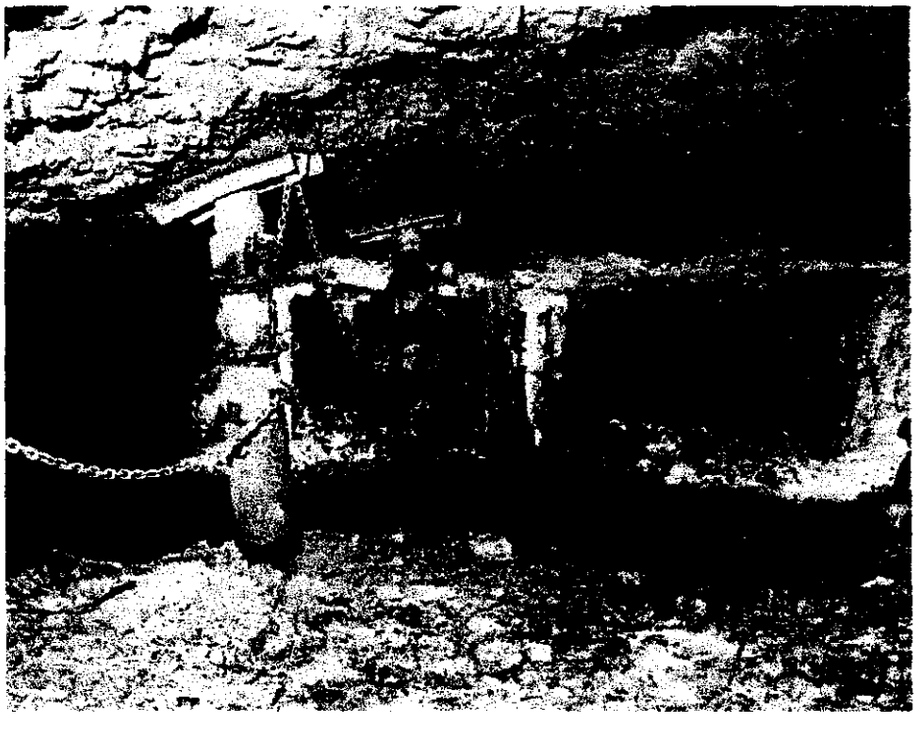

Figure 4. The face area of a typical tabular excavation in the South African gold mining industry. The stope face is towards the right. A typical stoping width is 1.2 m.

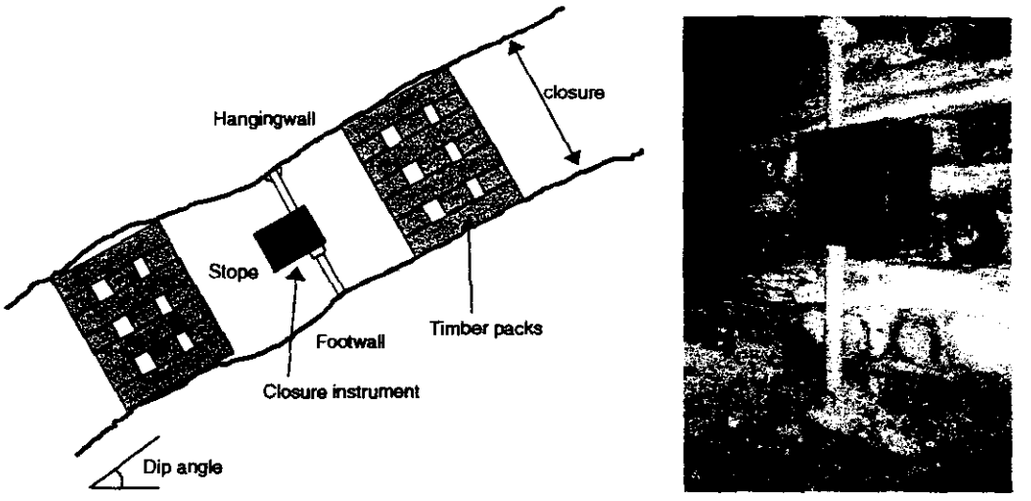

Figure 5. Installation of the closure instrument normal to the plane of the excavation.

The continuous closure data typically illustrates an instantaneous response at blasting time followed by a primary closure phase lasting approximately four to five hours and a steady-state closure phase (see Figure 6). After the next blast, this pattern is repeated. For tabular excavations in the Ventersdorp Contact Reef, the instantaneous response after blasting is very prominent, but it decreases rapidly in magnitude as the distance from the face to the measurement position increases. The steady-state closure rate also decreases in magnitude with distance to the face. For a distance of 4 m to 5 m from the face for an up-dip panel described in the thesis, the steady-state closure rate is approximately 2 mm/day. If all mining activity stops, this rate gradually decreases, but can still be as high as 0.2 mm/day after two weeks. Typical closure behaviour of the Ventersdorp Contact Reef is illustrated in Figure 6.

In contrast, for stopes in certain areas of the Vaal Reef, the steady-state closure rate can be as high as 15 mm/day. For these excavations, the instantaneous closure response at blasting time is very small. This is illustrated in Figure 7. Unlike the Ventersdorp Contact Reef, the steady-state closure rate of the experimental panel in the Vaal Reef increases with increasing distance to the face. This behaviour is probably caused by bedding plane separation in the hangingwall towards the back area of the panel.

Of significance is that the continuous closure measurements of tabular excavations in the Vaal Reef and Ventersdorp Contact Reef indicate that the time-dependent movements are much larger than typically expected for excavations in hard rock.

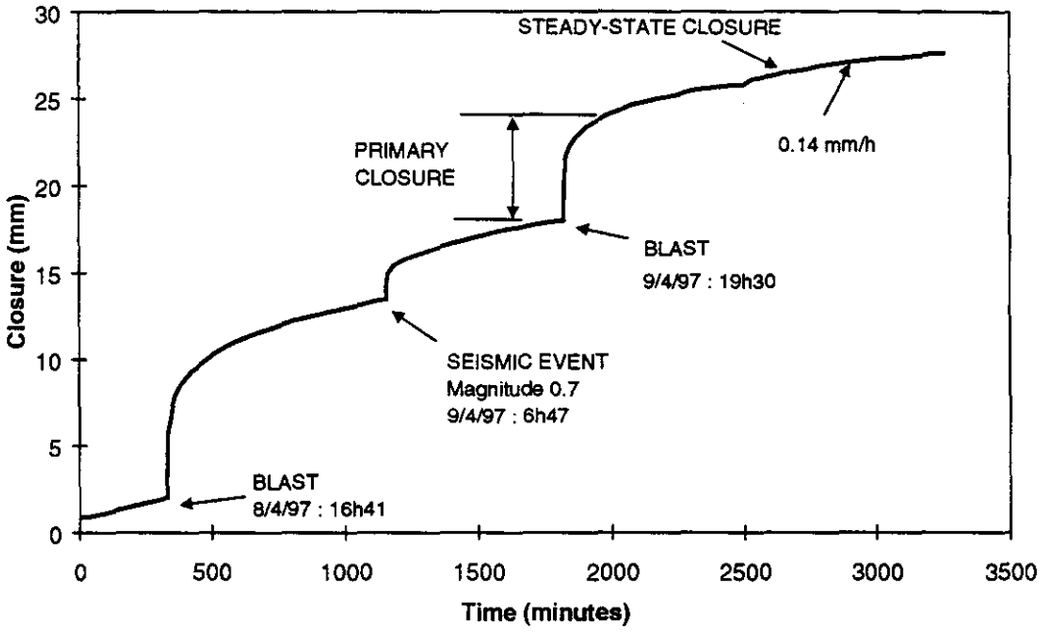

Figure 6. Typical time-dependent stope closure of the Ventersdorp Contact Reef at Western Deep Levels Mine. The steady-state closure rate was calculated for the period from approximately 600 minutes after the blast on 9/4/97 until the end of the data set.

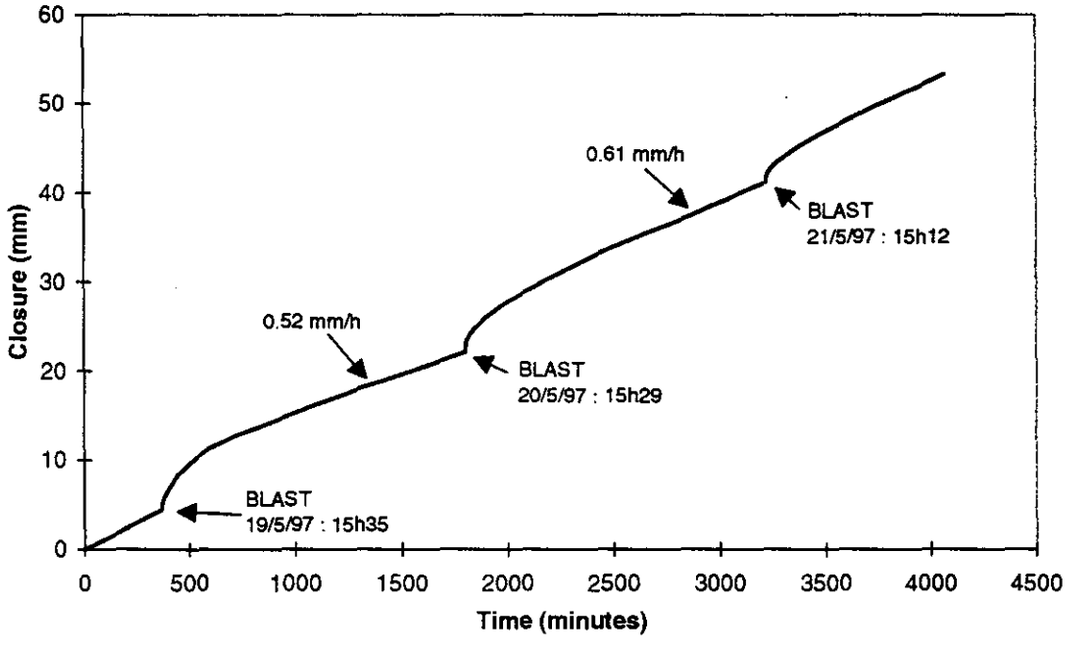

Figure 7. Typical closure profiles measured at Hartebeestfontein Mine. The steady-state closure rates were calculated for the periods from approximately 600 minutes after the blast until the next blast occurred.

4. Development of a viscoelastic convergence model for tabular excavations

As a preliminary attempt to simulate the time-dependent closure measured underground, a viscoelastic approach was investigated. Although this theory is unable to simulate the fracture zone around excavations, it appears attractive owing to its simplicity. As viscoelastic theory is still frequently used in rock mechanics, it was necessary to investigate the potential of this theory for simulating the time-dependent closure of tabular excavations. As no analytical model for the closure of tabular openings in viscoelastic media is available, a two-dimensional closure solution for a parallel-sided tabular stope in a viscoelastic medium was derived by the author. The solution was obtained by subjecting a known elastic solution to the viscoelastic correspondence principle. A particular viscoelastic model consisting of a certain combination of elastic and viscous elements also had to be selected as a building block. Solutions were derived for the Kelvin model, a three parameter model and the Burgers model. An important feature of this analytical solution is that it accounts for the incremental enlargement of these stopes. The two-dimensional closure solution for a single parallel-sided tabular stope (Figure 8) in a Burgers viscoelastic material (Figure 9) mined in n increments with both mining faces blasted simultaneously are given in equations [1] and [2]. The various coefficients in these two equations are given in equations [3] to [12].

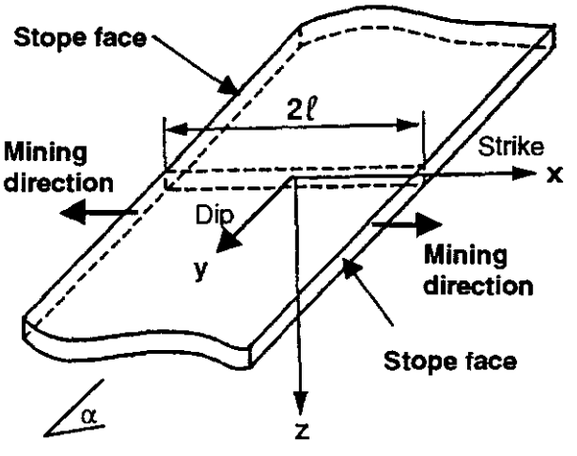

Figure 8. A single parallel-sided tabular stope. The analytical viscoelastic closure solution was derived for the two-dimensional section in the figure. The origin of the co-ordinate system is at the centre of the stope.

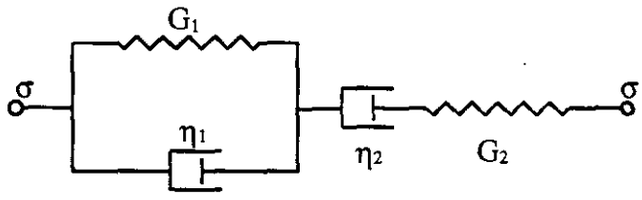

Figure 9. Representation of the Burgers viscoelastic model with the viscosity coefficients η_1 and η_2 and shear moduli G_1 and G_2.

$$S_z = \left\{ \sum_{i=1}^{n-1} \left[S_z(\ell_i, t-\tau_i) \right] - \left[S_z(\ell_i, t-\tau_{i+1}) \right] \right\} + S_z\left[\ell_n, t-\tau_n \right] \quad \text{for} \quad \tau_n < t \le \tau_{n+1} \quad [1]$$

where

$$S_z(\ell_i, t-\tau_i) = -4W_z \sqrt{\ell_i^2 - x^2}\ (1+\frac{dx}{2}) \quad \times$$

$$g_1 \left[1 + c_5 t + c_6 e^{-f(t-\tau_i)} + \left\{ c_7 \sinh b(t-\tau_i) + c_8 \cosh b(t-\tau_i) \right\} e^{\frac{-h(t-\tau_i)}{2}} \right] \quad [2]$$

and

$$W_z = \frac{-\rho g H}{2} \left[(1+k) + (1-k)\cos 2\alpha \right] \quad [3]$$

$$d = \frac{\sin\alpha \cos\beta}{H} \quad [4]$$

$$b = \sqrt{\frac{(6Kp_1 + q_1)^2 - 24K(6Kp_2 + q_2)}{4(6Kp_2 + q_2)^2}} \quad [5]$$

$$g_1 = \frac{2Kp_1q_1 + q_1^2 - 2Kq_2}{4Kq_1^2} \quad [6]$$

$$c_5 = \frac{2Kq_1}{2Kp_1q_1 + q_1^2 - 2Kq_2} \quad [7]$$

$$c_6 = \frac{2K(p_2q_1^2 - p_1q_1q_2 + q_2^2)}{q_2(2Kp_1q_1 + q_1^2 - 2Kq_2)} \quad [8]$$

$$c_7 = \frac{q_1^2(-12Kp_2q_1 + 6Kp_1q_2 - q_1q_2)}{2b(6Kp_2 + q_2)^2(2Kp_1q_1 + q_1^2 - 2Kq_2)} \quad [9]$$

$$c_8 = \frac{q_1^2 q_2}{(6Kp_2 + q_2)(-2Kp_1 q_1 - q_1^2 + 2Kq_2)} \quad [10]$$

$$f = \frac{q_1}{q_2} \qquad h = \frac{6Kp_1 + q_1}{6Kp_2 + q_2} \quad [11]$$

$$p_1 = \frac{\eta_1 G_2 + \eta_2 G_1 + \eta_2 G_2}{2G_1 G_2} \qquad p_2 = \frac{\eta_1 \eta_2}{4G_1 G_2} \qquad q_1 = \eta_2 \qquad q_2 = \frac{\eta_1 \eta_2}{2G_1} \quad [12]$$

where S_z is the stope closure, $2\ell_i$ is the span of the stope after mining increment i, ρ is the density of the rock, x is the position in the stope, g is the gravitational acceleration, H is the depth below surface, k is the ratio of horizontal to vertical stress, α is the dip of the reef, β is the angle between the x-axis and the dip, ν is Poisson's ratio, E is Young's modulus, n is the number of increments, t is time and τ_i is the time when increment i is mined. The Burgers viscosity coefficients η_1 and η_2 and shear moduli G_1 and G_2 are defined in Figure 9.

This equation was further modified to allow parameter calibration for stopes where only one face is mined at a time. It should also be noted that this solution is only valid for stopes where a two-dimensional approximation is possible and where no contact between footwall and hangingwall occurs in the centre of the stope. This viscoelastic closure model appeared to be promising as a good fit with experimental closure data was obtained. This is illustrated in Figure 10.

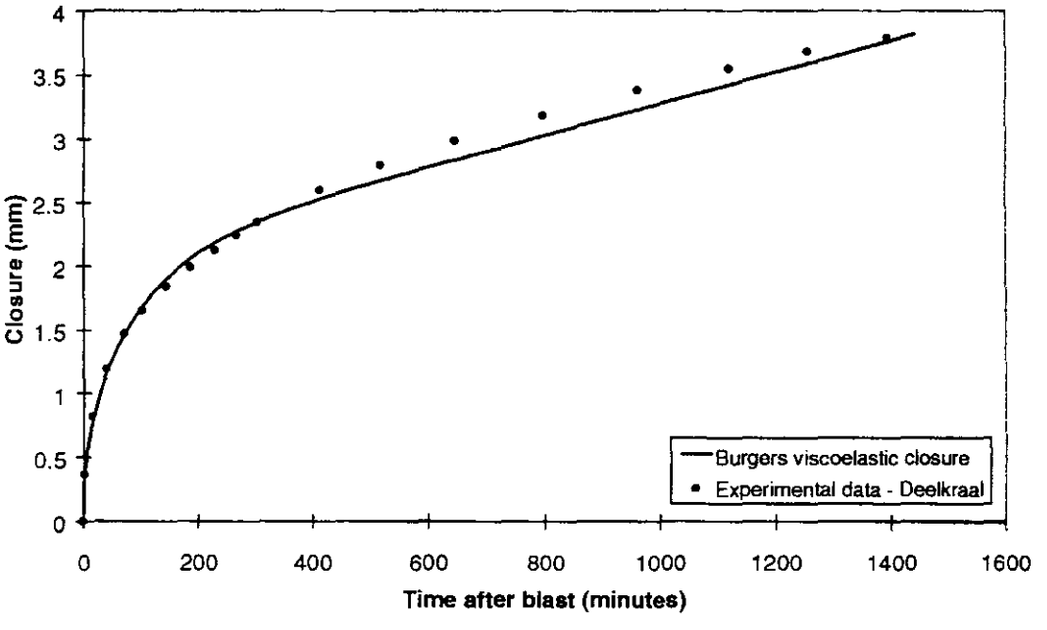

Figure 10. The Burgers viscoelastic closure solution fitted to experimental closure measured at Deelkraal Mine.

To complement the analytical solution, a two-dimensional displacement discontinuity method to solve incremental mining problems in a viscoelastic material was also developed by the author. It was, however, found that there are subtle problems with the use of viscoelastic theory in simulating the behaviour of tabular excavations. For the solution described above, the rate of steady-state closure increases with an increase in the distance to the face. This is opposite to what is measured underground in the Ventersdorp Contact Reef stopes. The problem arises due to the inability of viscoelasticity to simulate the formation of the fracture zone. This is not readily apparent when applying viscoelastic theory to circular tunnels in hard rock. For the special geometry of tabular excavations, however, calibration at a particular distance from the face does not necessarily give the correct closure rates at other positions. In spite of these problems, the viscoelastic solution might still be useful to simulate the closure rate at a particular point to assist in the design of appropriate support.

5. The applicability of a continuum viscoplastic model

From earlier work and the observations and modelling in this study, it became clear that the time-dependent failure processes in the rock play a prominent role in the time-dependent behaviour of deep excavations in hard rock. The significant time-dependent effects are confined to the fracture envelope surrounding the excavations. Previous workers showed that the far field rock mass behaviour can be adequately represented by elastic theory. An idealisation of this concept is given in Figure 11. Note that the actual shape of the fracture envelope is not necessarily as depicted in the figure.

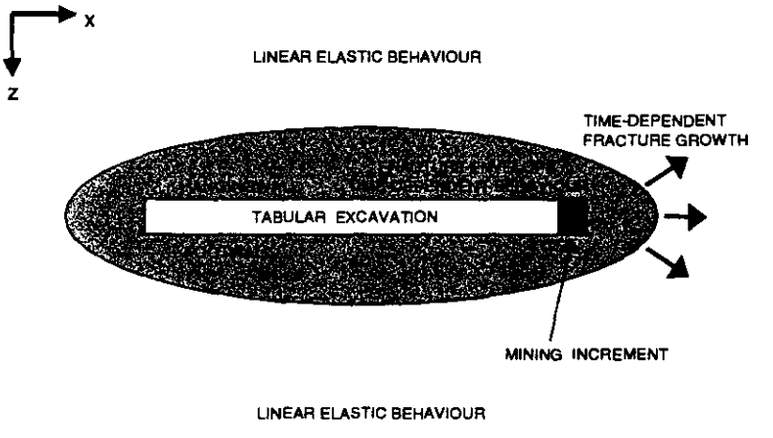

Figure 11. Conceptualization of the fracture zone surrounding tabular excavations (section view) and time-dependent extension of this zone following a mining increment.

To simulate the time-dependent fracture processes, the author developed a continuum elasto-viscoplastic model with a novel time-dependent weakening rule. This was implemented in a finite difference computer code. In this model, the intact rock behaves elastically, while a Mohr-Coulomb yield function determines the failure strength. Similar to classical viscoplasticity, the viscoplastic strain rate $\dot{\varepsilon}_i^{vp}$ after failure is given by

$$\dot{\varepsilon}_i^{vp} = \mu\langle f_s(t)\rangle \frac{\partial g_s}{\partial \sigma_i} \qquad \text{for} \quad i = 1, 2, 3 \qquad [13]$$

where μ is the fluidity parameter, g_s is the plastic potential function, $f_S(t)$ is the yield function and σ_i is a principal stress. A constitutive description of time-dependent rock behaviour needs to include the effect of strength degradation with time and/or deformation. Observations of time-dependent fracturing ahead of tabular stopes and in some haulages in the South African mines show that the rock becomes progressively more fractured with time, resulting in the gradual loss of cohesive strength in a particular volume of rock. This loss of strength was modelled by assuming that the rate of cohesion reduction $\dot{C}_c$ is proportional to the excess stress above the residual target surface.

$$\dot{C}_c = k_c\langle f_{res}\rangle \qquad [14]$$

where k_c is the cohesion decay factor and

$$f_{res} = \sigma_1 - \sigma_3 N_{\phi r} + 2C_r\sqrt{N_{\phi r}} \qquad [15]$$

$$N_{\phi r} = \frac{1+\sin\phi_r}{1-\sin\phi_r} \qquad [16]$$

is the residual target surface with C_r the residual cohesion and ϕ_r the residual friction angle. The principle embodied in equation [14] is based on the laboratory creep experiments described in Section 2 which indicated that if the rock specimens are loaded close to their failure strength, the creep rate and eventual creep failure occur faster than for a low stress. For a particular volume of rock under high stress, creep fractures will therefore form more rapidly, resulting in a faster loss of cohesion in the rock than for low stress.

The model described above was used to simulate the time-dependent increase in the extent of the fracture zone around squeezing tunnels at Hartebeestfontein Mine. In the numerical model, soon after development of the tunnel, the failed zone covered those areas where the stresses exceeded the failure strength of the intact rock. Time-dependent processes lead to gradual loss of residual strength in the fractured rock, transferring stress to the unfailed rock. This then also becomes fractured resulting in a time-dependent increase in the extent of

fracture zone. Depending on the chosen model properties, an equilibrium position is eventually reached with no further growth in the fracture zone.

To investigate the applicability of the model to simulate time-dependent stope closure, the incremental mining of a stope was investigated. Behaviour similar to that noted for the experimental results of the Ventersdorp Contact Reef was obtained. The incremental jump in closure after blasting is reduced as the distance to face increases. Furthermore, the closure rate of the steady-state phase also decreases into the back area. These results were encouraging as this behaviour cannot be simulated with a viscoelastic model as described above. Figure 12 illustrates the comparison between experimental closure data and the continuum elasto-viscoplastic model. No attempt was made to simulate the Vaal Reef as the behaviour of this reef is dominated by the bedding plane movements. The finite difference mesh is not suitable for the inclusion of multiple discontinuities to simulate these parallel bedding planes. To simulate the time-dependent behaviour within an assembly of explicit discontinuities, a discontinuum viscoplastic model suitable for implementation in a boundary element code was developed as described in Section 8.

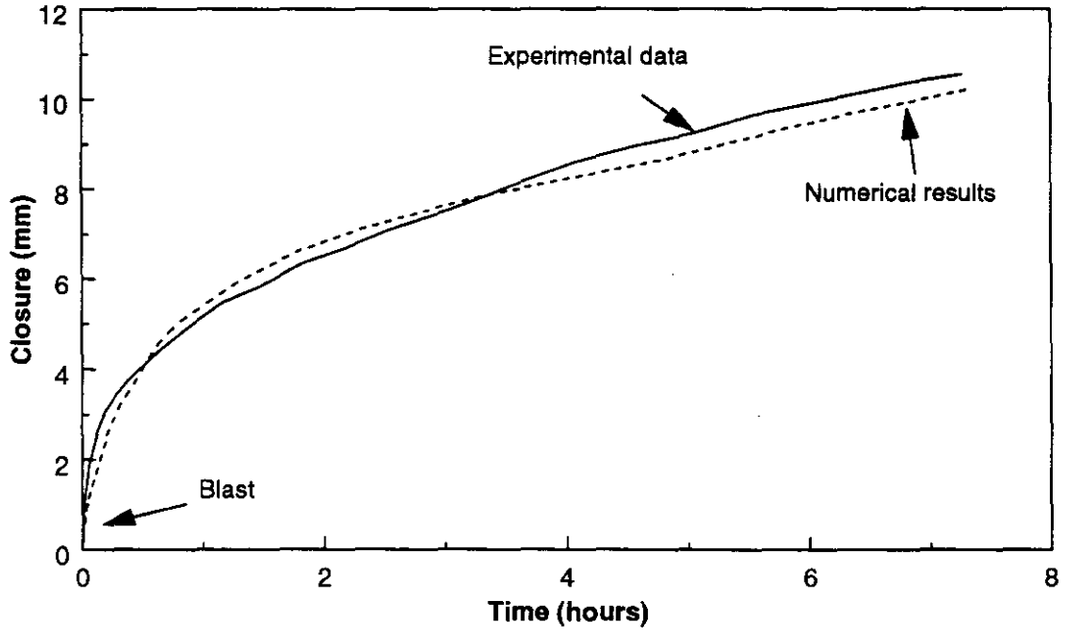

Figure 12. Experimental and simulated stope closure after blasting.

6. Continuous closure data as a diagnostic measure of face stress

When comparing typical results of the Vaal Reef stope in Figure 7 with those of the Ventersdorp Contact Reef stope in Figure 6, it is clear that significant differences exist between these different geotechnical areas. For a more direct comparison, typical closure increments after blasts for the two areas are plotted in Figure 13. The two experimental sites

are approximately at the same depth and for these specific data sets, the closure instruments were approximately the same distance from the face. Although care should be taken when comparing these sites directly, owing to different mining geometries, the following important differences are noted. The closure behaviour of the Ventersdorp Contact Reef is characterised by a large instantaneous jump after blasting followed by a low closure rate. These areas also appear to be prone to face bursting. In contrast, for the Vaal Reef, the closure is characterised by a small instantaneous jump after blasting followed by a high rate of closure. The risk of face bursting is lower in these areas, although the risk of falls of ground is pronounced.

The author postulated that the instantaneous jump in closure after blasting is the result of the immediate redistribution of stress following the removal of an increment of rock in the face. The more significant the disturbance to the stress field, the more pronounced the immediate response will be. If the increment of rock removed by blasting carries no load (in essence loose rock lying at the face) no change in the stress field will take place and no change will be noticed in the closure behaviour. The instantaneous closure response after blasting therefore appears to indicate the role the removed rock played in maintaining the stress equilibrium before the blast. For the Ventersdorp Contact Reef, the significant instantaneous closure after blasting is probably an indicator of a more highly stressed face area than the Vaal Reef. This may explain why face bursting appears to be more pronounced on this reef than the Vaal Reef.

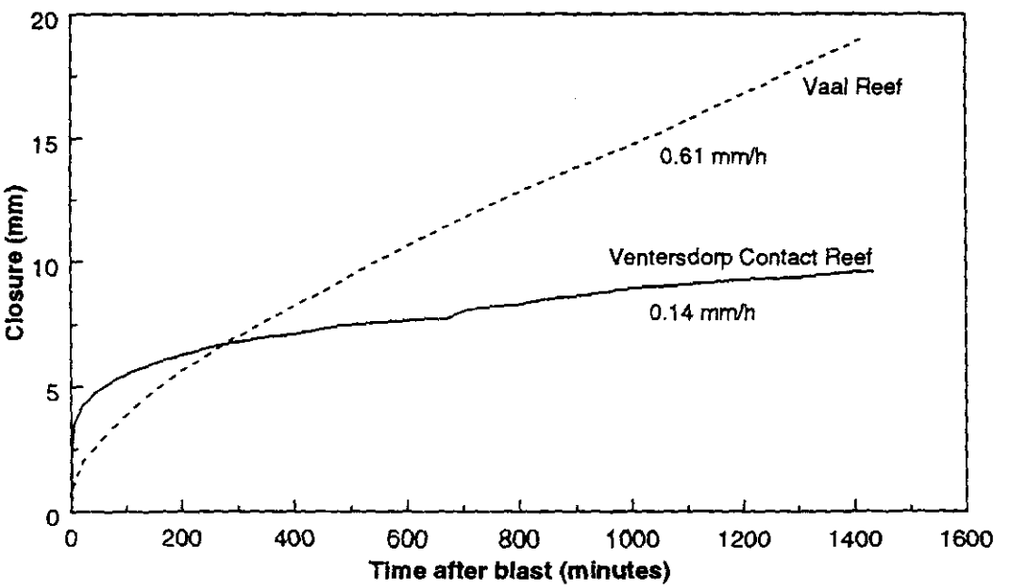

Figure 13. Comparison of typical closure profiles of the Ventersdorp Contact Reef and Vaal Reef.

A further difference between these areas is the high rate of steady-state closure of the Vaal Reef stopes compared to the Ventersdorp Contact Reef stopes. The high steady-state closure rate is an indication of efficient stress redistribution through mobilization and growth of the fracture zone and slip on discontinuities such as the bedding planes. This in turn may result in low face stresses. The large time-dependent behaviour of the fracture zone, however, leads to a rapid deterioration of hangingwall conditions increasing the risk of falls of ground.

From the arguments above, it appears that the instantaneous closure after blasting may be an indication of the proximity of the stress peak to the face. This hypothesis was tested by simulating two stopes (A and B) using the viscoplastic model described in Section 5. The only difference between these stopes is a different rate of cohesion decay. This resulted in the rock ahead of the face of Stope B losing its strength much faster than the rock ahead of Stope A and therefore carrying less load. This is illustrated in Figure 14 where the major principle stress is plotted against distance ahead of the original face position just before an increment is mined. For Stope A the peak is closer to the face. The next increment of mining will remove the first metre of rock thereby forcing the stress carried by this increment to be instantaneously redistributed. As the average stress in this increment of rock is larger for Stope A than Stope B, it is expected that the instantaneous closure will be bigger for A. This is confirmed by the closure that followed this increment in Figure 15. The steady-state closure for Stope B is larger as the failed rock loses its strength faster resulting in greater time-dependent deformation.

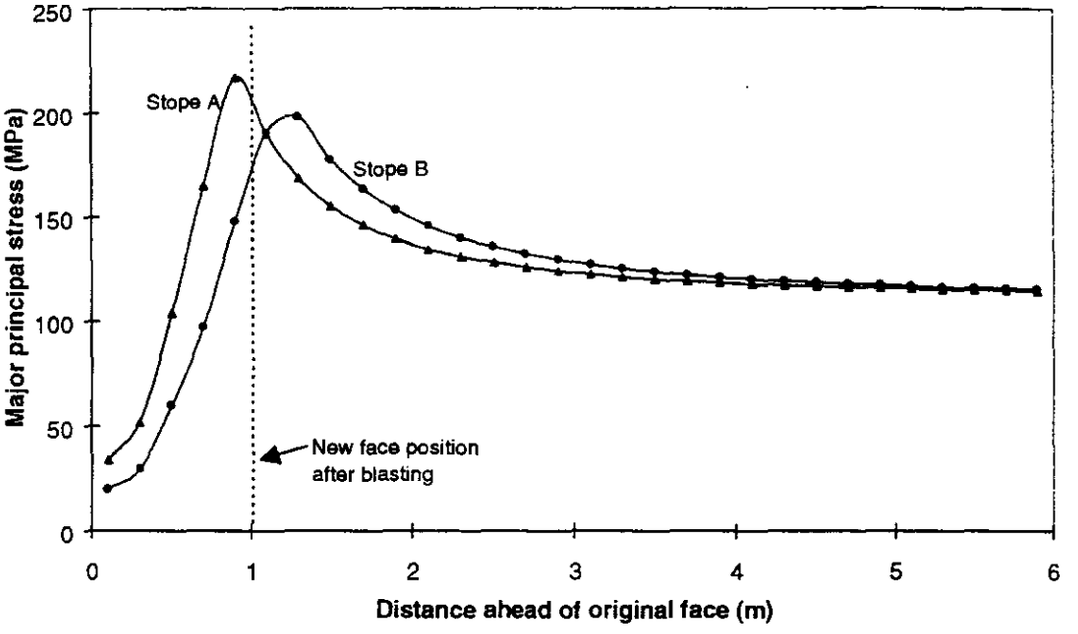

Figure 14. Major principal stress as a function of distance ahead of the face for two simulated stopes before the blast.

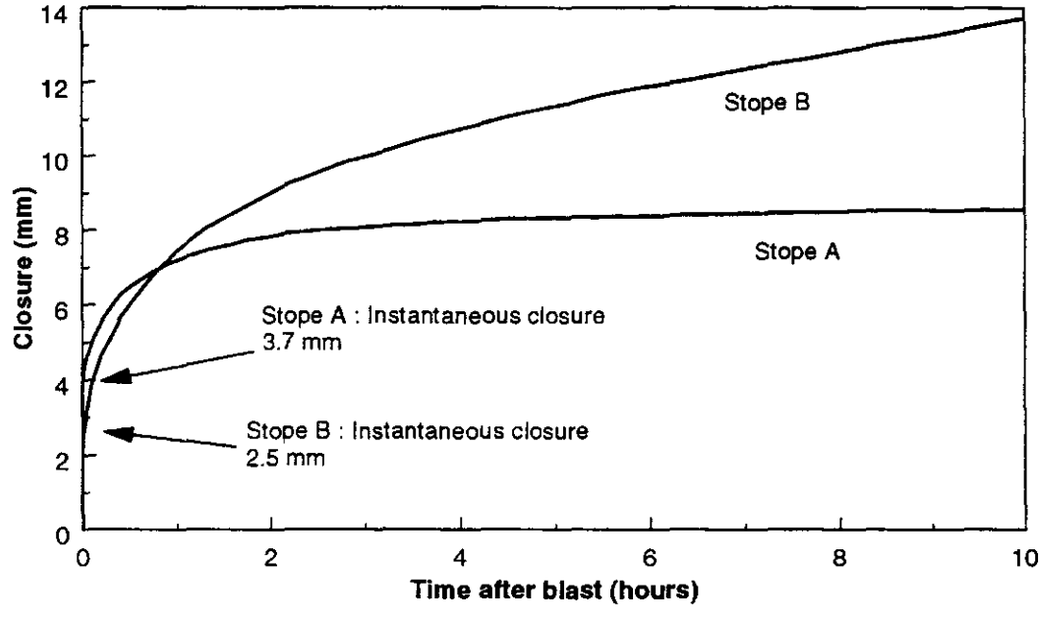

Figure 15. Comparison of the simulated closure behaviour as a function of time after the blast. The measurement position was 0.5 m behind the original face.

These results have significant practical implication as, in future, the continuous closure measurements might be developed as a hazard indicator.

7. Laboratory investigation of discontinuity creep

The shear creep of discontinuities is currently poorly understood. As the shear creep of bedding planes or other large discontinuities appear to play a role in the observed time-dependent behaviour, a laboratory testing program was initiated to investigate this phenomenon. As no suitable testing equipment was available, a creep shear box was developed in which the displacement transducers could be mounted directly on the sides of the rock specimen (Figure 16). This prevented the data from being obscured by creep components of the equipment or resin castings used to mount the samples.

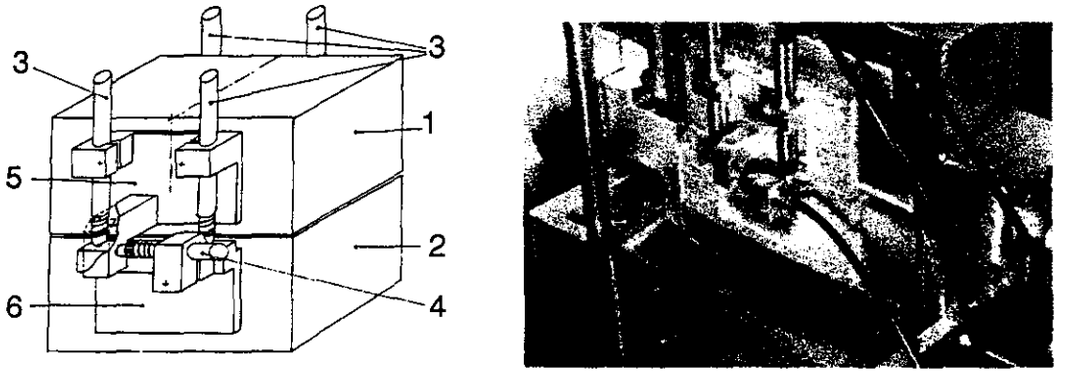

Figure 16. Details of the creep shear box developed for this study. The displacement transducers are attached directly to the discontinuity specimen. 1) Top half of the shear specimen, 2) Bottom half of the shear specimen, 3) Displacement transducers for measuring vertical displacements, 4) Displacement transducers for measuring horizontal displacements, 5) Upper fixing plate, 6) Lower fixing plates.

From the preliminary tests, it became clear that discontinuity creep of hard rock can be divided into two groups, namely creep of discontinuities with gouge infilling and creep of discontinuities with matching surfaces and no infilling. Mining induced extension fractures that have not been subjected to previous shear displacements (belonging to the second group) do not undergo appreciable shear creep. This is illustrated in Figure 17. The testing methodology consisted of applying an appropriate constant normal stress to the sample and increasing the shear stress in a stepwise fashion with a period of 24 hours between load increases. This was continued until the shear strength of the discontinuity was exceeded.

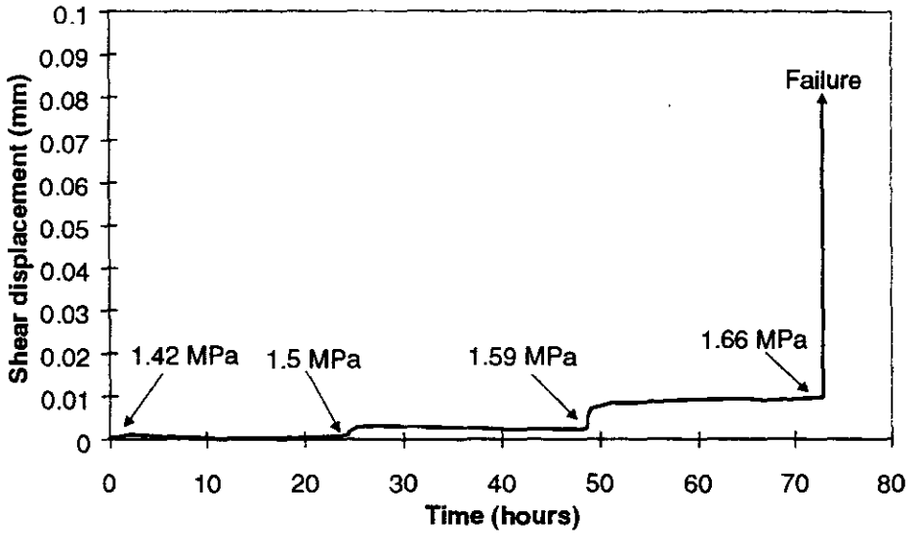

Figure 17. Shear creep behaviour of a mining-induced extensile fracture in Ventersdorp lava for a stepwise increase in shear stress. The normal stress was 1 MPa. The shear stress magnitudes are given in the figure. The sample was tested at a constant humidity of 50 % and a temperature of 22 °C.

For those discontinuities with thick infilling, significant creep displacement was observed. Both artificial gouge and gouge collected from underground were tested. Typical primary and secondary behaviour is noted (Figure 18). The primary shear creep phase includes a prominent instantaneous response that is not recoverable and increases for larger shear stress/shear strength ratios (Figure 19). The magnitude of the creep rate in the secondary phase also increases for higher shear stress/shear strength ratios (Figure 20). A stress power law is proposed to simulate this behaviour. The creep rate is, however, not only a function of the shear stress/shear strength ratio but also of the absolute stress magnitudes. It also depends on the humidity and the gouge thickness with a faster creep rate for a thicker gouge infilling. A rheological model with stress-dependent parameters was developed in the thesis to simulate the behaviour described above.

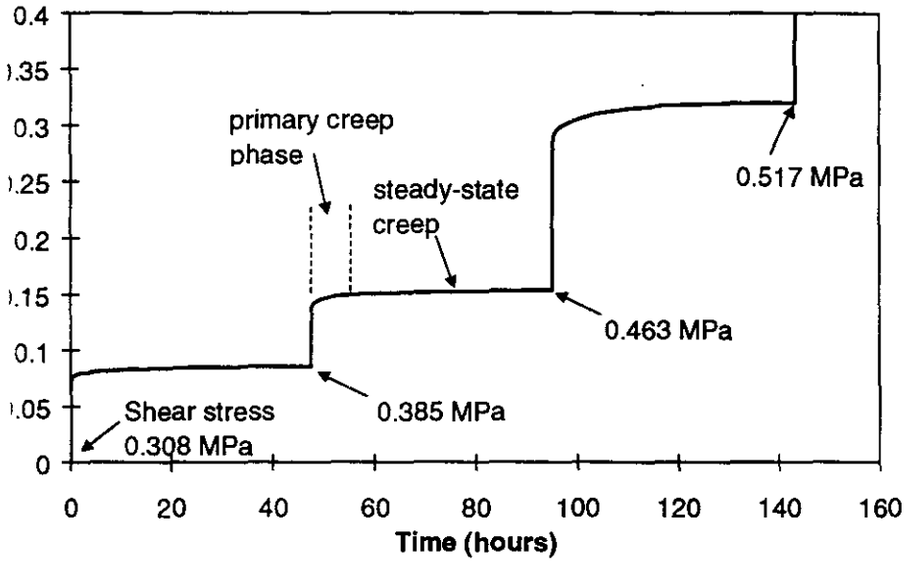

Typical shear creep behaviour of the sawcut discontinuity with gouge infilling wise increase in shear stress. The normal stress remained constant at 1 MPa. The kness was 2 mm and the humidity and temperature was controlled at 50 % and ctively.

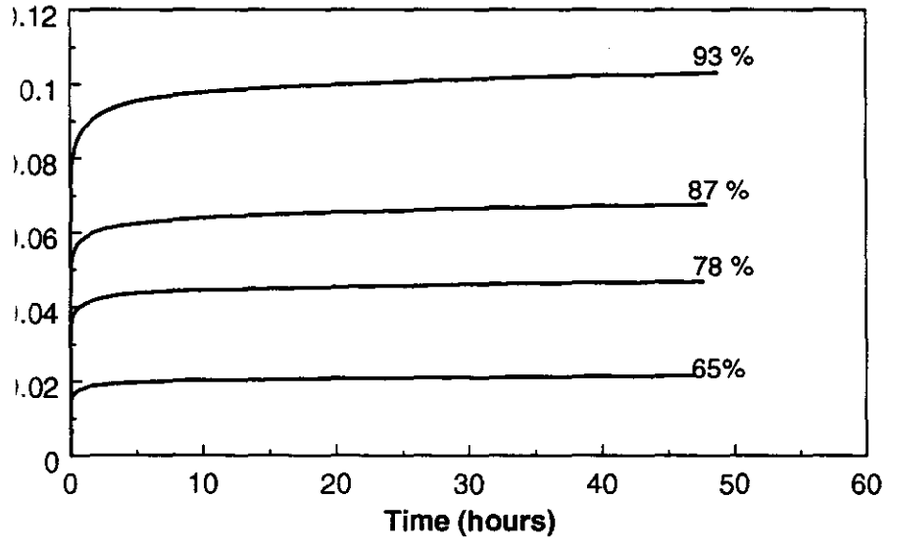

The effect of shear stress magnitude on the creep behaviour for a gouge-filled ty. The percentages indicate the magnitude of the shear stress relative to the gth (0.276 MPa). The normal stress was 0.5 MPa and the gouge thickness 2 mm.

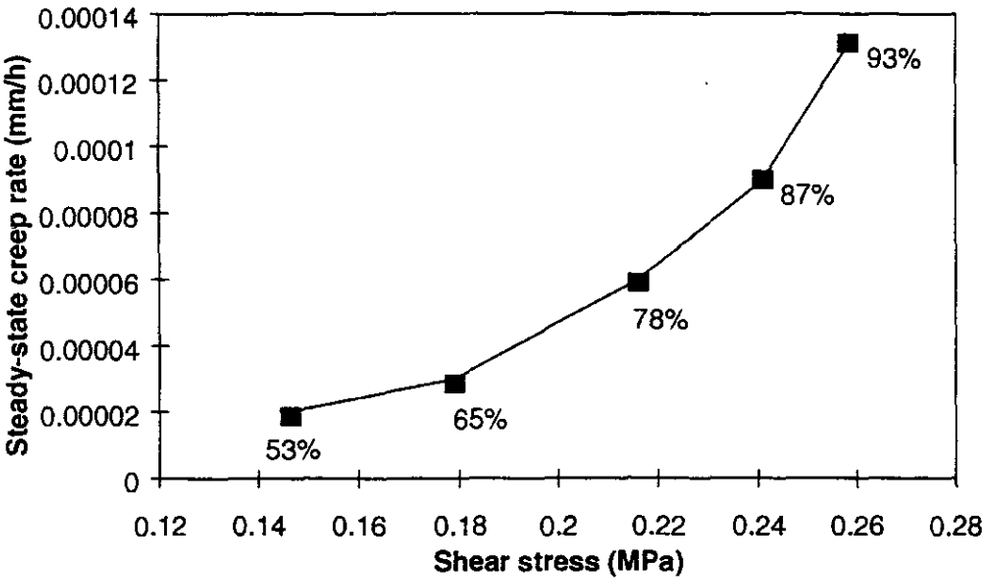

Figure 20. The effect of shear stress magnitude on the steady-state creep rate for a gouge-filled discontinuity. The percentages indicate the magnitude of the shear stress relative to the shear strength (0.276 MPa). The normal stress was 0.5 MPa and the gouge thickness 2 mm.

8. A proposed discontinuum model for the time-dependent behaviour of hard rock

Although the continuum viscoplastic model described in Section 5 can simulate the time-dependent behaviour of the fracture zone, it cannot be used if the behaviour is dominated by major discontinuities such as the creep of bedding planes. For these cases, a discontinuous viscoplastic formulation implemented in a displacement discontinuity boundary element program was developed. It was postulated that the intact rock material behaves in an elastic fashion and that all inelastic behaviour, including viscoplastic effects, is controlled by the presence of multiple interacting discontinuities. In this approach, explicit slip is modelled as a time-dependent (but not elastodynamic) process and progressive redistribution of stress can occur near the edges of mine openings both as a function of time and in response to changes to the size of the openings.

The developed discontinuum viscoplastic formulation is analogous to continuum viscoplasticity. The rates of change in normal and shear discontinuity are assumed to be given by

$$\begin{Bmatrix} \frac{\dot{D}_S}{d} \\ \frac{\dot{D}_N}{d} \end{Bmatrix} = \mu\langle F\rangle \begin{Bmatrix} \frac{\partial Q}{\partial \tau} \\ \frac{\partial Q}{\partial \sigma_n} \end{Bmatrix} \qquad [17]$$

where D_S and D_N are the local shear and normal components of the displacement discontinuity vector, F is the yield function (a Mohr-Coulomb yield function is assumed in this study), Q the plastic potential function, τ the shear stress acting on the discontinuity, σ_n the normal stress and μ is the fluidity. It is postulated that the viscoplastic effects are limited to a finite discontinuity thickness d. This thickness not only includes gouge width and asperity heights but also the thin layer of rock adjacent to the discontinuity wall controlling the strength and deformation properties. The intact rock between discontinuities behaves elastically. This formulation was implemented in a displacement discontinuity program with an appropriate time-stepping solution scheme.

Stope modelling was undertaken by covering the problem space with a random mesh or tessellation of viscoplastic discontinuities. Figure 21a shows a typical distribution used. This distribution should be considered as potential fracture surfaces. These fractures are initially intact with a prescribed strength determined by the failure criteria. For this preliminary modelling, no bedding planes were included. Owing to computer memory limitations, the number of elements was limited. The object of this modelling was therefore to study the effect of the time-dependent fracture process and not replicating observed fracture patterns. Mining was undertaken in an incremental fashion, allowing the progressive evolution of the fracture zone.

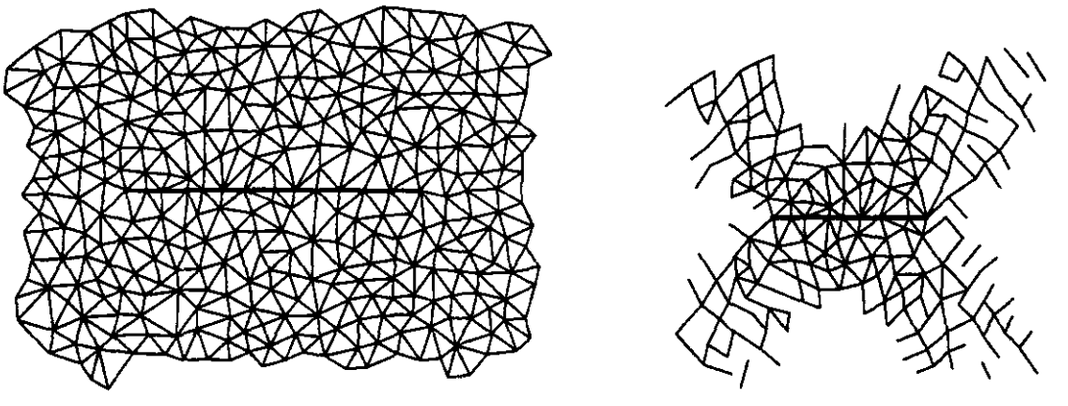

(a) (b)

Figure 21. a) Initial random distribution of potential fracture planes surrounding the future stope. b) Development of the fracture zone 24 hours after the 9th mining increment. The stope is represented by the thick black line.

Figure 21b illustrates the development of the fracture zone 24 hours after the 9^{th} mining increment. The discontinuities shown are all those mobilised up to that particular point in time. An important consequence of the prescribed viscoplastic behaviour is that the additional fracturing caused by a sudden increase in stress occurs in a time-dependent fashion. After a mining increment, the existing discontinuities surrounding the stope are subjected to an increase in mining induced stress. Those discontinuities subjected to stresses above the yield surface relax in a time-dependent fashion according to equation [17]. This relaxation process causes a stress transfer to the solid rock at the edge of the fracture zone. New fractures then form in these positions as a time-dependent process. For the example above, the increase in cumulative fracture length as a function of time after a blast is illustrated in Figure 22. It should be emphasised that there are no changes in the excavation dimension during this time period. Similarly to underground observations, the majority of new fractures formed within a short period after the blast, and the rate of fracturing then diminished until the next blast. Also plotted in Figure 22 is the typical rate of cumulative seismicity after production blasts showing similar trends.

The time-dependent fracture process leads to the typical stope closure profile illustrated in Figure 23. Similar to the results in Section 3, the highest rate of closure occurs after blasting time and this decays until the next blast takes place. If the discontinuities are subjected to a time-dependent decrease in cohesive strength, an increase in closure is observed in the longer term.

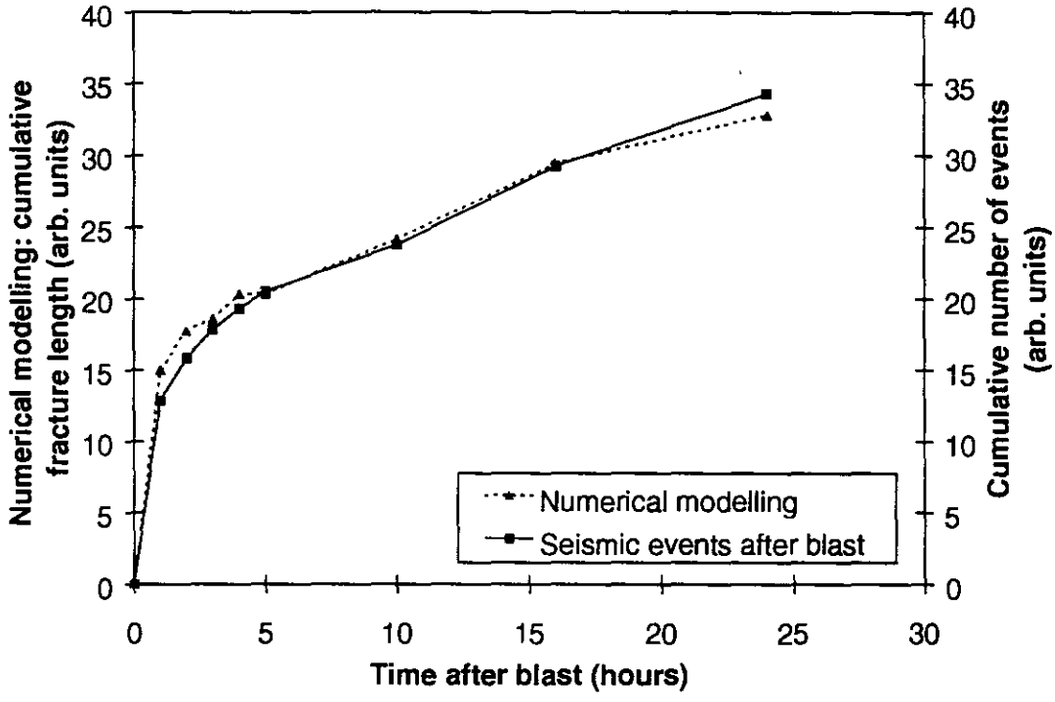

Figure 22. Increase in cumulative fracture length after the 9th mining increment. The typical rate of seismicity after production blasts is also plotted showing similar trends.

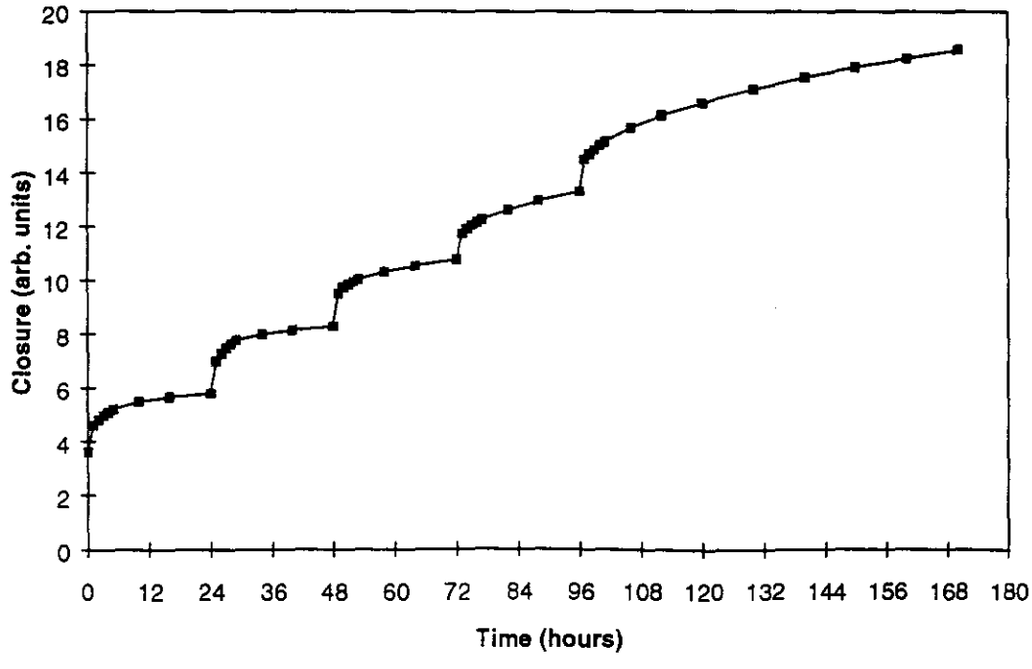

Figure 23. Numerical stope closure as a function of time. Blasting took place at 0, 24, 48, 72 and 96 hours.

9. Conclusions and practical implications

This study investigated the time-dependent behaviour of hard brittle rock around deep level excavations. Underground closure measurements in the stopes of the deep South African gold mines indicated a significant time-dependent response of the rock mass. Laboratory experiments showed that this behaviour cannot be explained by the creep of intact rock alone. The observed time-dependent behaviour is a result of the rheology of the fracture zone surrounding these excavations. The time-dependent extension of the fracture zone ahead of the working faces after blasting operations is an important mechanism controlling the observed closure behaviour. The creep of major discontinuities such as bedding planes also plays a role. A shear creep testing program was conducted in the laboratory using specially designed and constructed shear creep equipment. The preliminary results indicated that discontinuities with gouge infilling undergo noticeable shear creep while the creep rate for mining induced extension fractures in hard rock is negligible. To simulate the time-dependent behaviour of deep tabular excavations, the author investigated the following analytical and numerical approaches.

a) **Viscoelasticy**: Analytical viscoelastic solutions for the time-dependent closure of a tabular excavation mined in incremental steps were derived. A viscoelastic displacement discontinuity program to solve incremental problems in viscoelasticity was also developed. Although these models give a good fit with measured stope closure at a particular point in the stope, the calibrated solution does not necessarily give the correct results for other distances from the stope face. This is a result of the inability of viscoelastic theory to simulate the fracture zone around these excavations.
b) **Continuum elasto-viscoplasticy**: A model based on classical viscoplasticity was developed and implemented in a finite difference code to simulate the formation of the fracture zone and the time-dependent behaviour of this zone. A novel time-dependent weakening rule was used to simulate the loss of cohesion in the near-field rock mass due to delayed fracture formation. This model proved successful in simulating the time-dependent stress transfer processes ahead of tabular excavations and the resulting time-dependent closure behaviour of the stopes. It was also used to simulate the squeezing behaviour of some tunnels in these deep mines. The drawback of this continuum approach is its inability to simulate behaviour that is dominated by the creep of major discontinuities such as bedding planes.
c) **Discontinuum viscoplasticity**: A discontinuum viscoplastic approach was developed and implemented in a displacement discontinuity boundary element code. This allows explicit

crack growth and development of these fractures in a time-dependent fashion. This approach was successful in simulating the time-dependent behaviour of the fracture zone around tabular excavations and the resulting time-dependent closure behaviour. The advantage of this model over the continuum approach is the ability to easily include bedding planes and the associated creep of these structures.

Practical implications of this research

1. The developed viscoplastic models allow the study of the effect of mining rate on the stability of the fracture zone and the position of the stress peak ahead of stope faces in deep hard rock mines.
2. Squeezing conditions in the deep hard rock tunnels can also be simulated with these models to determine optimum support strategies.
3. The improved understanding of the time-dependent closure behaviour of deep tabular stopes will lead to better stope support design and a quantification of the effect of time of support installation.
4. It appears that continuous closure data in tabular stopes provides useful diagnostic information about the stress conditions in the fracture zone ahead of the stope face. In future, this may be developed into a hazard indicator to identify conditions such as areas prone to face bursting.